Analys av vågförhållanden under 1872-stormen (Backafloden)

Analysis of the wave conditions during the 1872 storm

Emmy Sukchaiwan[1], Anna Adell[2], Caroline Hallin[2], Björn Almström[2]

[1] Sweco Sverige AB, Drottningtorget 14, 211 25 Malmö, Sweden emmy.sukchaiwan@sweco.se
[2] Division of Water Resources Engineering, Lund University, John Ericssons väg 1, 223 63 Lund, Sweden

Sammanfattning

Stormfloden 1872, i Sverige även känd som Backafloden, är den största kända stormfloden som drabbat södra Östersjön. Den representerar ett händelseförlopp där extrema vattenstånd uppstod på grund av en ovanlig kombination av vindförhållanden, vilket orsakade omfattande kustöversvämningar. Denna studie presenterar vågförhållandena under stormen 1872, simulerade med vågmodellen SWAN och baserat på rekonstruerade vinddata. Vågklimatet har analyserats och jämförts med befintliga vågdata (1959-2023) för fyra specifika platser längs Skånes syd- och östkust. Under stormens kulmen nådde de simulerade signifikanta våghöjderna 3,5, 3,6 och 4,1 m längs sydkusten och 5,7 m vid östkusten. Detta innebär att förhållandena under 1872 stormen överstiger de typiska extrema våghöjderna för hälften av de undersökta platserna. Resultaten visar på den värdefulla information och kunskap som sällsynta historiska stormhändelser kan bidra med, vilket utgör ett viktigt komplement till befintliga data. De resultat som presenteras i denna studie möjliggör att inkludera nivåerna under 1872 stormen för bättre riskbedömningar vid design av kustskydd och klimatanpassningsåtgärder i kustzonen.

Abstract

The 1872 storm, in Sweden also known as Backafloden, is the largest known storm surge recorded in the southern Baltic Sea. It represents an event where extreme surge levels were generated due to an unusual combination of wind conditions, causing widespread coastal flooding. This study presents the wave conditions during the 1872 storm, simulated using the SWAN model forced with reconstructed wind data. The wave climate has been analyzed and compared with existing long term hindcast wave data (1959-2023), in four specific coastal locations distributed along the south and east coast of Scania. During the peak of the storm, simulated significant wave heights reached 3.5, 3.6 and 4.1 m, respectively along the south coast and 5.7 m at the east coast. This means that the peak conditions during the 1872 storm surpass the typical extreme wave heights for half of the investigated locations. The findings highlight the valuable information that extreme and rare historical events can provide and serve as an addition to existing records. The data and results presented in this study offer the potential to include the levels during the 1872 storm for improved risk assessments for coastal infrastructure and communities.

Keywords: Storm surge, Wave modelling, SWAN, Baltic Sea, Backafloden

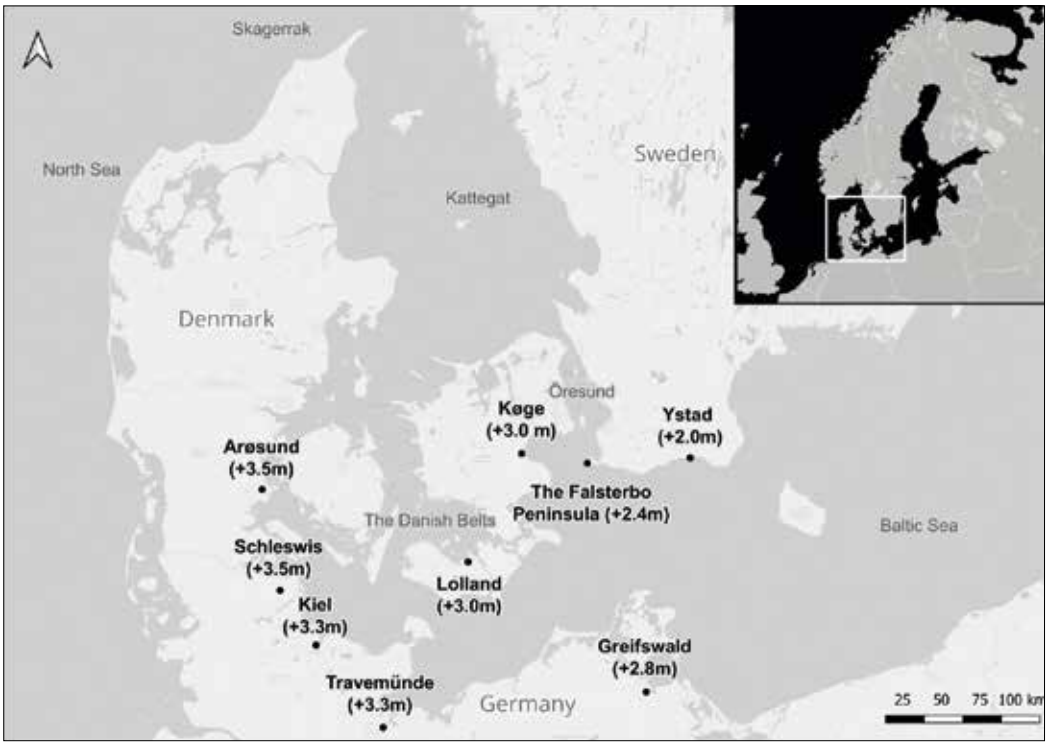

Figure 1. Overview of the southern Baltic Sea with peak water levels along the Swedish, Danish and German coast during the 1872 storm. The water levels (rel. MSL) are based on the study of Hallin et al. (2021).

Introduction

Coastal hazards, such as erosion and flooding, are largely related to storms and the associated storm surges. High water levels (storm surge) in combination with large waves may result in loss of land and flooded hinterlands. When occurring simultaneously, storm surges enforce the wave impact on the coast, exacerbating the potential for damage and destruction. High water levels can impact the coastline, as they allow larger waves to reach the shore. These larger waves, in turn, contribute to the erosion process. Additionally, the presence of larger waves can further elevate the water levels through wave setup and wave runup, which can result in increased overtopping and flooding. Risk assessments and design of coastal protection often rely on extreme scenarios with return periods far exceeding the length of the observational records of wave buoys and water level gauges. To supplement the relatively short records, historical storms that occurred before systematic observations can provide valuable information. With modern tools for wave climate and water level simulation, these historical storm events can be reconstructed and utilized in risk analyses. This enables a more comprehensive understanding of coastal hazards and allows for more accurate assessments.

The 1872 storm, known as Backafloden in Sweden, is the largest known storm surge in the southern Baltic Sea (Jensen & Müller-Navarra, 2008). According to Colding (1881), the entire southern part of the Baltic Sea was impacted by the storm surge. There are several studies assessing the water level dynamics (Bruss, et al., 2009) as well as waves (Aakjær & Buch, 2022) during the event. However, the emphasis of those studies has been on the Danish and German Baltic Sea coasts. Along the Swedish coast, the conditions are not exactly known due to the lack of observation stations. Fredriksson et al. (2016) estimated the maximum storm surge level at the Falsterbo Peninsula using anecdotal information and an old flood-memory stone. The maximum water level during the 1872 storm was estimated to be +2.4 m

(rel. MSL), see Figure 1. However, there have been no studies investigating the wave conditions along the south coast of Sweden.

To fill this knowledge gap, this study aims to assess the wave conditions during the 1872 storm along the south coast of Sweden. The study utilizes a regional hindcast SWAN (Simulating Waves Nearshore) model forced with reconstructed wind data from the event. The results are then compared with the decadal hindcast wave climate for the period 1959 to 2023 (Adell, et al., 2023) to assess the severity of the wave conditions during the 1872 storm. A comprehensive understanding of the 1872 storm is crucial as it is the largest storm surge known in the region. A basic understanding of a storm includes knowledge about extreme water levels and wave heights since both parameters greatly influence the extent of potential coastal flooding and erosion.

Background

The Baltic Sea is a semi-enclosed body of water, connected to the North Sea through Öresund and the narrow Danish Belts (Figure 1). This connection limits the exchange of water between the two seas. However, strong northwesterly and westerly winds can cause infilling of the basin increasing the mean water level with up to 0.5 m (Hünicke, et al., 2015). Westerly winds can also push water to the east part of the Baltic Sea basin. This results in water levels being low on the southwestern coastlines during the predominant westerly storm events. Approximately 24 hours after the storm has passed, these water masses return to the southwestern coastlines, leading to an increase in water levels. This phenomenon is known as seiche (Hanson & Larson, 2008).

Figure 2 presents the time series of available measured water levels at Skanör-Falsterbo from 1992 until 2024. The highest observed water level in the entire record is 1.53 m which occurred in January 2017. The dashed horizontal line in Figure 2 represents the maximum water level at the Falsterbo Peninsula during the 1872 storm which is estimated to +2.4 m (Hallin, et al., 2021), meaning that it is 0.9 m higher than the highest observed level in the tide gauge record.

Waves within the Baltic Sea are predominantly wind-generated. The study by Adell et al. (2023) showed that in the southern Baltic Sea, the annual cumulative wave energy from the western sector typically dominates over the eastern sector. This dominance is related to the prevailing westerly winds over the region, However, the study also identified years when eastern wave energy was more prominent, suggesting that while easterly storms are less frequent, they can occur in the area. The behaviour is associated with the alternating positive and negative phases of the North Atlantic Oscillation (NAO).

Meteorological conditions influence both the water level variation and the wave conditions in the southern part of the Baltic Sea. However, it is important to note that the factors driving extreme values

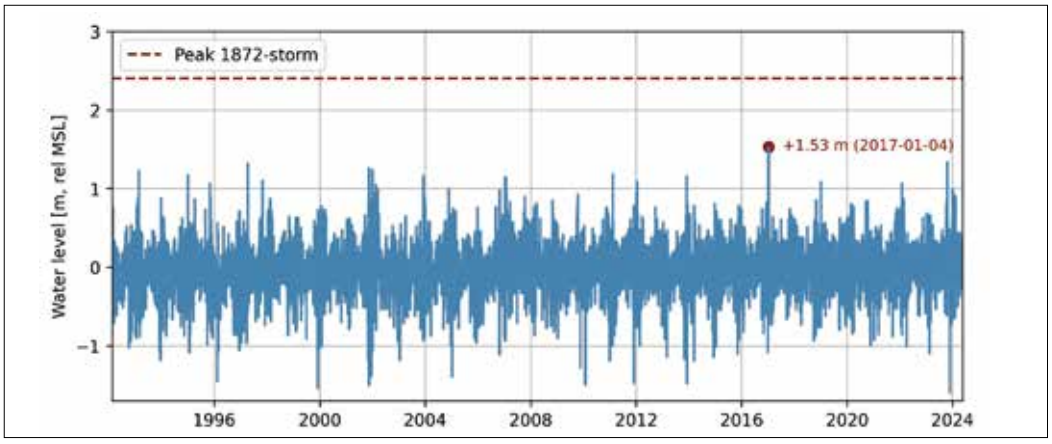

Figure 2. Measured water levels (rel. MSL) at the Skanör-Falsterbo station from 1992 till 2024 (blue) and the estimated water level at the Falsterbo Peninsula during the peak of the 1872 storm (red).

for these parameters are different (Hanson & Larson, 2008). This indicates that different meteorological conditions drive extreme water levels compared to those responsible for extreme wave heights. To illustrate this, the measured water level in Skanör-Falsterbo was analysed alongside the one hourly simulated significant wave height extracted at 10 m depth outside the Falsterbo Peninsula (Sukchaiwan, 2023), for the period 1959 till 2023. Table 1 shows the five highest measured water levels along with the dates they occurred and the corresponding simulated peak significant wave heights. Conversely, Table 2 presents the five highest simulated significant wave heights and the associated peak water levels. These tables show that while the region does experience both high water levels and large wave heights, these phenomena typically do not occur simultaneously. However, it is worth noting that there is one storm event, Babet, where there is a combination of extreme water levels and wave heights. Babet occurred on October 20, 2023, and it represents the most extreme wave height hindcast for the period 1959 till 2023. Whereas the water level during the event ranks as the fifth highest level.

Table 1. Highest measured water level and corresponding simulated peak significant wave height at the Falsterbo Peninsula.

Date	Water level (rel. MSL, m)	Significant wave height (m)
2017-01-04	1.53	1.0
2023-10-21 (Babet)	1.34	3.6
1997-04-11	1.32	1.2
2001-11-16	1.26	0.5
2002-01-02	1.24	0.9

Table 2. Highest simulated significant wave height and corresponding measured peak water level at the Falsterbo Peninsula.

Date	Significant wave height (m)	Water level (rel. MSL, m)
1999-12-03	3.7	0.73
2023-10-21 (Babet)	3.6	1.34
2013-12-05	3.5	0.44
1993-01-14	3.4	0.49
2002-02-22	3.4	0.53

The 1872 storm

The reconstruction of the atmospheric conditions during the 1872 storm by Rosenhagen and Bork (2009) showed a complex interplay of atmospheric systems that resulted in the extreme storm event. The initial phase of the storm was dominated by westerly winds, which pushed water from the North Sea into the Baltic Sea. Subsequently, the atmospheric condition shifted, and intense easterly winds developed. On November 13, these winds escalated to a hurricane force, due to the significant air pressure gradient over the southern Baltic Sea. These winds induced significant amounts of water being pushed to the southwestern basin of the Baltic Sea, which were further amplified by the occurrence of seiches within the basin. The combination of easterly winds and seiches resulted in an abnormal rise in water levels on the southwestern coast of the Baltic Sea, while simultaneously causing a drop in water levels on the eastern coasts. The peak water levels reached +2.4 m (rel. MSL) on the Swedish coast (Figure 1), while on the German and Danish coast, an even higher water level of +3.5 m (rel. MSL) was observed according to Hallin, et al. (2021). On top of the high-water levels, the hurricane-force easterly winds also generated extreme waves that coincide with the extreme storm surge. This indicates that the storm was a rare event, as the simultaneous occurrence of extreme waves and water levels is unusual in the southwestern Baltic Sea (Hanson & Larson, 2008).

This catastrophic event caused significant loss of lives, extensive property damage, and destruction of boats in Germany, Denmark, and Sweden. In Sweden, the low-lying Falsterbo Peninsula was severely flooded and on the Swedish East coast people were swept offshore by the large waves and drowned. Germany and Denmark were even worse affected with several hundred fatalities and several villages that were obliviated (Hallin, et al., 2021).

Method

This study utilized a regional hindcast wave model (Adell, et al., 2023) for the southern Baltic Sea and the reconstructed wind during the 1872 storm (Rosenhagen & Bork, 2009).

The wave model setup

The wave climate was simulated using the numerical model SWAN with cycle III version 41.31a (Booij, et al., 1999). The SWAN model is widely used, and applicable to a range of scales from local to regional (Hashemi, et al., 2015; Pallares, et al., 2014; Rusu, et al., 2008). The model is a third-generation spectral wave model that was developed to simulate wind-generated waves and swells in both deep water and nearshore areas The deep-water processes are represented in the energy transfer from the wind to the waves, dissipation of wave energy due to whitecapping, and nonlinear energy transfer through quadruplet interaction between the waves. The shallow-water processes are represented by energy dissipation through bottom friction, depth-induced wave breaking and energy transfer due to non-linear triad interaction.

The SWAN model was used in the study of Adell et al. (2023) to hindcast the wave climate for the southern Baltic Sea, with detailed resolution specifically for the south coast of Sweden, for the period 1959 to 2021. Since the initial release, the time series has been extended until December 2023. Additionally, for the purpose of this analysis, the temporal resolution has been increased from three hours to one hour. The study utilized the ERA5 global reanalysis dataset for the wind input, which is a comprehensive assimilation of model data and observations on a global scale (Hersbach, et al., 2020). The model domain covers the southern Baltic Sea, Öresund, Kattegat and Skagerrak regions, see Figure 3. To ensure the model's accuracy, Adell et al. (2023) calibrated and validated the model against wave observation from buoys at 16 distinct locations. A strong correlation was found between the simulated significant wave heights and the observations, affirming the good performance of the model. Hence, this validated model setup was used in this study to hindcast the wave climate during the 1872 storm.

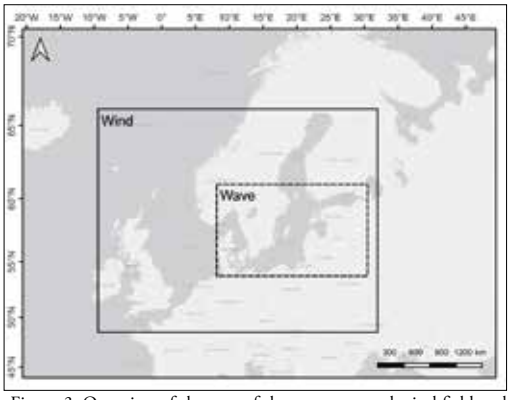

Figure 3. Overview of the area of the reconstructed wind field and the model domain of the SWAN wave model.

The computational grid varies in resolution, with a 25 km resolution applied in the offshore areas. Closer to shore, the grid resolution was decreased to 200 m in order to better describe the nearshore wave dynamics. The bathymetry data for offshore regions was obtained from EMODnet (EMODnet, 2021), with a resolution of 115 x 115 m. For the south coast of Scania, a more detailed bathymetry was available (Malmberg-Persson, et al., 2016). This bathymetry covers the nearshore area from 0-10 m depth with a resolution of 2 x 2 m.

Reconstructed wind data

The wind field during the 1872 storm was reconstructed by Rosenhagen and Bork (2009) from analyses of air pressure data and historical literature from the time of the storm. For their study, the observed air pressure and temperature were requested from the national meteorological services of Europe from more than 230 observation stations for the period November 1st to 13th in 1872.

The methodology employed by Rosenhagen and Bork (2009) involved the classical meteorological technique of calculating geostrophic winds from the pressure fields. These winds were then adjusted to represent wind conditions at a height of 10 m above ground using empirical methods. The reconstructed wind field accuracy was assessed by comparing the wind direction and speed from the nearest sea point on the reconstructed grid to observed values of coastal stations taken from the study of Baensh (1875).

Rosenhagen and Bork (2009) acknowledged that there were some discrepancies between the reconstructed data and the observed values. These deviations were attributed to the necessary standardization of the diverse air pressure data collected, the interpolation involved in the air pressure analysis, and the reliance on empirical methods to estimate wind conditions at 10 m above the surface. Despite these chal-

lenges, the reconstructed wind field was found to be in good agreement with the observed wind, validating the effectiveness of the reconstruction process.

The area of the reconstructed wind field, in Figure 3, covers a geographical range between latitudes 48.5° - 66.0° N and longitudes 9.5° W – 32.0° E. The data set includes wind direction and 10-meter wind speed, represented by u- and v-vectors, which are the standard meteorological components used to describe the wind. During the initial eleven days of the reconstruction period, the wind data was reconstructed three times a day, at 06, 14 and 21 UTC. However, on November 12th and 13th, the data were reconstructed four times a day: at 06, 08, 14 and 21 UTC. The increased frequency of data points over the last two days reflects the need for more detailed information during the peak of the storm event.

The available reconstructed wind field (Rosenhagen & Bork, 2009) was interpolated to create hourly values and modified to fit the extent compatible with the SWAN model domain. The hourly wind data depicted in Figure 4, illustrate both the wind speed and direction of the wind at the Falsterbo Peninsula. Initially, for the first ten days, the prevailing winds were from the west with moderate strength, but this shifted to strong northeasterly winds that reached a speed of 33.1 m/s on November 13th.

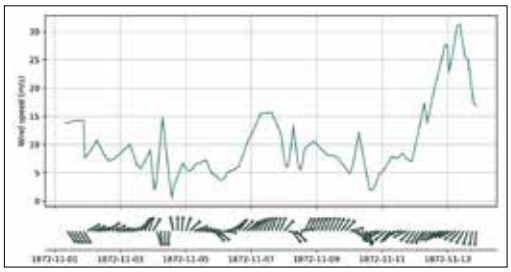

Figure 4. Time series of the reconstructed wind speed and direction at the Falsterbo Peninula.

Result

1872 storm wave climate

The wave climate was simulated for the period November 1st to 13th in 1872. Figure 5 shows the simulated wave conditions during the peak of the

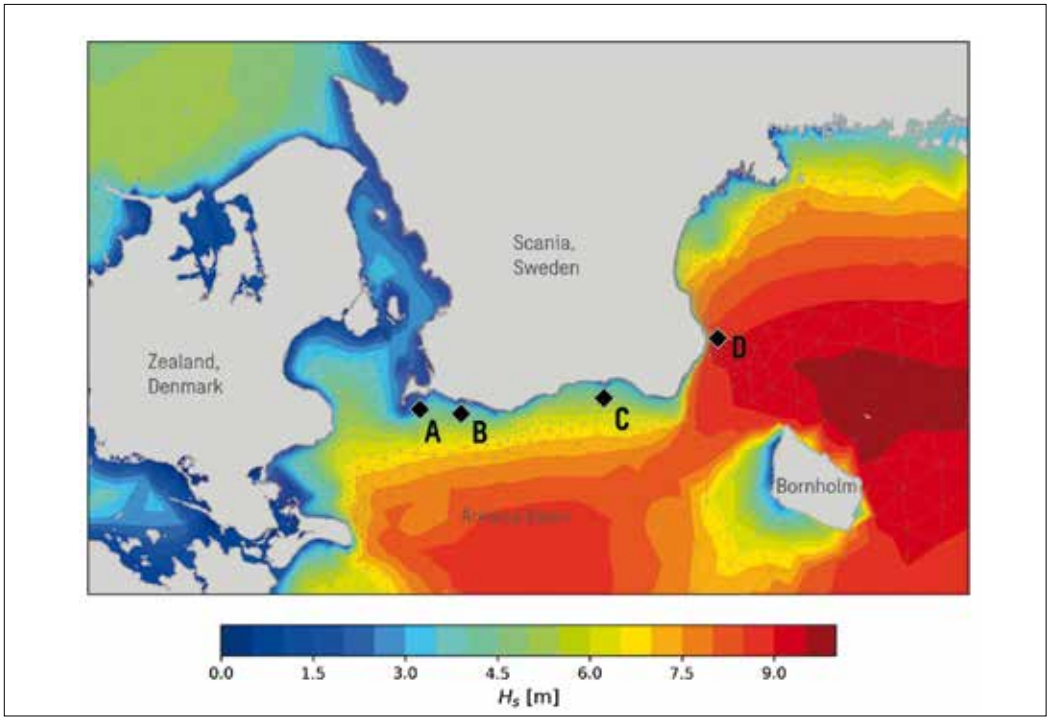

Figure 5. Simulated significant wave height [Hs] during the peak of the 1872 storm, with wave data extraction points (A, B, C, and D) along the south coast of Sweden.

storm, on 10 UTC November 13th,1872. The figure illustrates higher significant wave heights on the eastern coast of Scania in comparison to the southern coast. This difference in wave height can be attributed to the geometry and orientation of the coastline in relation to the storm direction, which affects the fetch length and how waves transform as they propagate towards the coast. The fetch length is a crucial factor for wave development. The fetch is defined as the uninterrupted distance over which the wind blows across the water. During the peak hours, the storm generated dominant northeasterly winds impacted the east coast of Scania. However, the south coast remained sheltered from these winds due to its geographical orientation, which does not directly face the northeasterly direction. As the wind generates waves in a specific direction, these waves refract as they approach the coast due to the bathymetry. Consequently, the wave height decreases as the waves refract. Therefore, the east coast experienced larger waves.

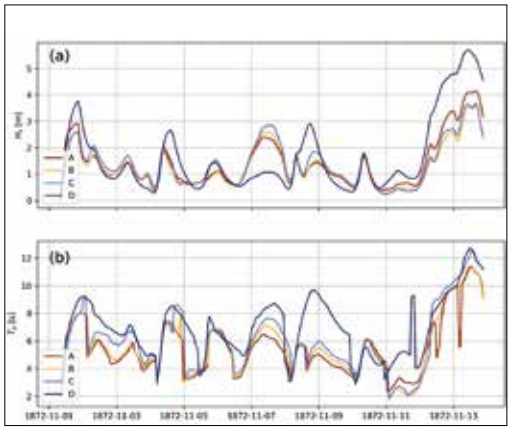

Figure 6. Time series of simulated significant wave height [Hs], given in top panel (a), and peak period [Tp], given in bottom panel (b), at location A, B, C, and D during the reconstructed period.

Figure 6 shows the time series of the simulated significant wave height and peak period at locations A, B, C and D along the Scanian coastline, representing offshore wave conditions at a depth of 10 m. Notable, during the peak of the storm, differences in significant wave height are simulated between locations A (4.1 m), B (3.5 m), C (3.6 m), and particularly location D (5.7 m). The variation of wave height can be attributed to the coastline orientation in relation to the prevailing wind direction.

Comparison with decadal hindcast wave climate

The wave climate during the 1872 storm was analysed and compared with the wave climate data simulated for the period from 1959 to 2023, as presented by Adell et al. (2023). This comparison is depicted in a scatter plot in Figure 7, the figure illustrates the relationship between the significant wave height and peak period at the four specific locations shown in Figure 5. The scatter plot shows that at locations A and D, the simulated significant wave heights during the 1872 storm surpassed those simulated for the 64-year reference period. Conversely, at locations B and C, the 1872 storm wave heights were found to be comparable with the highest values of the hindcast data within the same extended period. It should be noted that the extreme wave heights in the data series from 1959 to 2023 are typically generated by wind directions ranging from southeast to southwest.

In the Baltic Sea, waves with long peak periods are not commonly observed as the wave climate is dominated by wind-waves, as opposed to swell. However, Figure 7 reveals the presence of waves with peak periods exceeding 12 seconds. During the 1872 storm event, the wave conditions were extraordinary due to the unique combination of elevated wave heights and long peak periods. This combination contributed to the extreme wave condition during the storm event, distinguishing it from the typical wave climate experienced over the past six decades.

Discussion

In the Baltic Sea, high water levels and large waves are generally generated by different meteorological conditions and hence extreme levels of the two parameters typically do not coincide (Hanson & Larson, 2008). However, during the 1872 storm, there was a convergence of high-water levels and large waves, similar to the event known as Babet in October 2023. The conditions during the 1872 storm were more extreme than those during Babet, as the event was driven by an unusual combination of wind conditions. To understand the significance of this event, the simulated significant wave height during the 1872 storm was

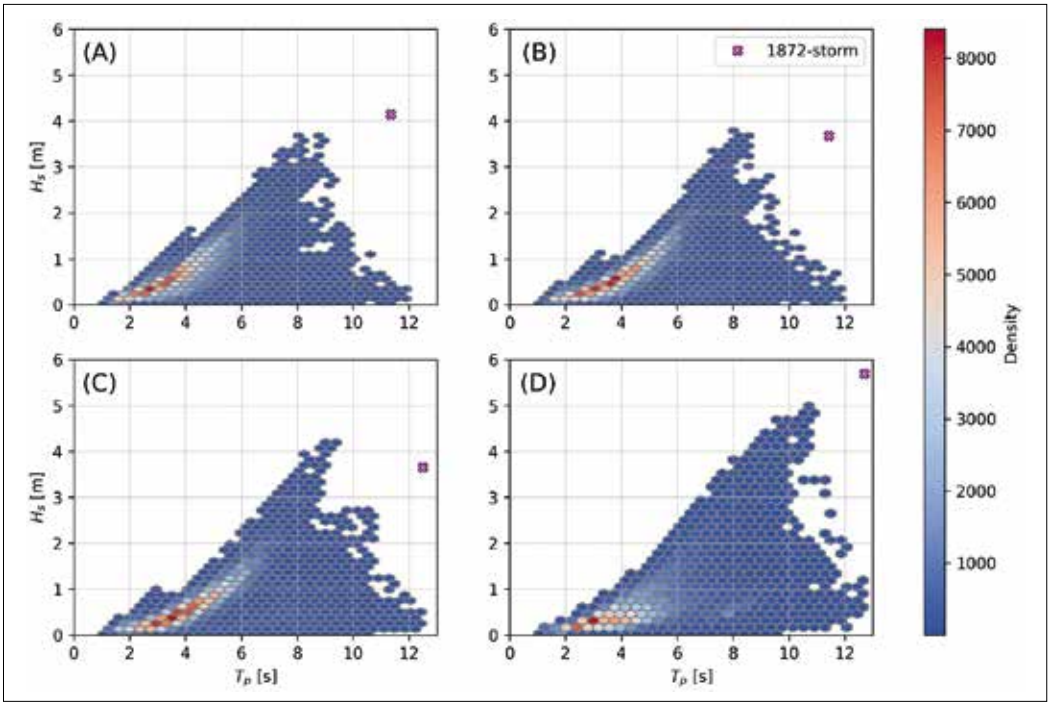

Figure 7. Combination of the significant [Hs] and peak period [Tp] at 10 m depth, during the period 1959-2023 at the four locations A, B, C and D, along the south coast of Sweden. The density of the dataset is indicated by the colour bar. The peak of the 1872 storm is shown in purple cross.

compared to the decadal hindcast wave data along the south coast of Sweden, from 1959 to 2023. The findings showed that the waves during the 1872 storm were distinct from typical extreme waves in the area. While the other extreme waves generated by winds with directions ranging from the southeast to the southwest (Adell, et al., 2023), the 1872 storm waves originated from northeasterly wind. Moreover, the combination of large wave heights and long peak periods (exceeding 12 seconds) during the storm event deviates from the typical wave climate. Waves with long peak periods usually only occur with small wave heights in the southern Baltic Sea.

The validation of the simulated significant wave height for the 1872 storm can be challenging due to the absence of historical wave observation data. However, a comparative analysis with other wave models offers a viable alternative for validation. Specifically, the simulated significant wave heights from this study can be compared with the results from the Danish Meteorological Institute's (DMI) wave model (Aakjær & Buch, 2022). The comparison of the simulated wave heights in the Arkona Basin, in Figure 5, from this study (7.5 – 9.0 m) and the wave heights produced by DMI's model (8.0 – 10.0 m) concludes that both sets of wave heights are similar. Small deviations between the two results can be reasonably attributed to differences in the wind data inputs and the wave models used for the simulations. Each model may process wind data differently and incorporate different physical formulations. Despite these differences, the magnitudes of the simulated wave heights are in good agreement, suggesting a reliable representation of the wave conditions during the 1872 storm.

The simulation of the wave climate during the 1872 storm only utilized the reconstructed wind data, which is an effective approach for simulating wave heights in deeper offshore waters where the effect of water level fluctuations on wave formation is minimal. However, in nearshore areas where the water depth is small, the dynamics between the waves and the seabed become increasingly important. Processes such

as shoaling, refraction, and breaking significantly affect wave behaviour as they approach the shore, and changes in water levels can greatly influence these processes. Only the water levels during the peak of the storm event were available (Hallin, et al., 2021) and no comprehensive reconstructed time series exist, therefore the water level fluctuations could not be included in the wave simulation. Despite this limitation, the results from this wave simulation can still serve as valuable boundary conditions for nearshore wave simulations at local level. By using the simulated wave heights from this study as boundary conditions, future studies can account for the effect of water level fluctuations, allowing for a more comprehensive understanding of wave behaviour during the 1872 storm in nearshore areas.

The impact of storm surges on coastal regions is a complex interplay between various factors, including the storm duration, storm surge level, and waves. The runup level which is crucial for assessing flood risk and coastal erosion, is the sum of the still water level, wave setup and wave runup height. Although historical records offer valuable insights into the total water level experienced during the 1872 storm, they lack specific details on the proportion attributable to the wave action. The analysis of measured water levels and simulated significant wave heights in the Falsterbo Peninsula shows that high total water level can be caused by either elevated water levels or large wave heights. The most extreme total water level scenario arises from the simultaneous occurrence of both. Although such simultaneous extremes are rare in the southern Baltic Sea, the 1872 storm provides a historical example of their high-impact consequences. This unique interplay during the 1872 storm underscores the importance of considering such extreme combinations in design levels to ensure adequate resilience and preparedness for similar events in the future. The obtained results of simulated significant wave heights from this study can be used to determine the wave runup and its contribution to the total water level. The information can be used for identifying vulnerable areas along the south coast of Sweden and gaining a comprehensive understanding of the potential extent of damage.

Conclusion

This study presents the simulated wave climate during the 1872 storm on the south coast of Sweden. The simulation utilized a regional SWAN model setup based on the work of Adell et al. (2023) and the reconstructed wind field of Rosenhagen and Bork (2009). Analysis shows that at several locations along the coast, the significant wave height during the 1872 storm surpassed those hindcast during a 64-year reference period (1959-2023). Furthermore, the comparison indicates that the extreme wave conditions during the storm, characterized by both large wave heights and long peak periods, are uncommon in the region. The conditions during the 1872 storm surge represent an extraordinary and rare combination of high-water levels and large wave heights. The study underscores the importance of considering such interaction for a more comprehensive evaluation of the risks associated with coastal flooding and erosion in the semi-enclosed Baltic Sea. The insights gained from this study can be valuable in further applications of the design of coastal protection and adaptation measures.

Acknowledgement

We would like to thank Gudrun Rosenhagen and Ingrid Bork for their contribution to this study by providing the reconstructed wind data. The reconstructed wind data not only provided us with the necessary inputs for our wave model but also enhanced our understanding of the 1872 storm and its impact on the southern Baltic Sea region.

Aakjær, P. & Buch, E., 2022. The 1872 super-storm surge in the Baltic–the Danish perspective.. Die Küste, 92.

Adell, A. o.a., 2023. Spatial and temporal wave climate variability along the south coast of Sweden during 1959–2021 Regional Studies in Marine Science, 63, p. 103011..

Baensch, O., 1875. Die Sturmfluth an den Ostsee-Küsten des Preussischen Staates vom 12./13. November 1872. Zeitschrift für Bauwesen, Berlin.

Booij, N. R. R. C., Ris, R. C. & Holthuijsen, L. H., 1999. A third-generation wave model for coastal regions: 1. Model description and validation. Journal of geophysical research: Oceans, 104(C4), pp. 7649-7666.

Bruss, G. o.a., 2009. Design scenarios for coastal protection structures on the german baltic sea coast. u.o., u.n., pp. 3593-3605.

Bugajny, N. &. F. K., 2022. Defining a single set of calibration parameters and prestorm bathymetry in the modeling of volumetric changes on the southern Baltic Sea dune coast.. Oceanologia, 64(1), pp. 160-175.

Clemmensen, L. B. o.a., 2014. Morphological records of storm floods exemplified by the impact of the 1872 Baltic storm on a sandy spit system in south-eastern Denmark. Earth Surface P rocesses and Landforms, 39(4), pp. 499-508.

Colding, A., 1881. Nogle undersøgelser over stormen over Nord- og Mellem-Europa af 12th -14th november 1872 og over den derved fremkaldte vandflod i Østersøen. Videnskabernes Selskabs Skrifter, 6. Række, naturvidenskabelig og matematisk afdeling, p. 245–304.

EMODnet, 2021. Emodnet bathymetry.

Fredriksson, C., Tajvidi, N., Hanson, H. & Larson, M., 2016. Statistical analysis of extreme sea water levels at the Falsterbo Peninsula, South Sweden. Journal of Water Management and Research, 72, pp. 129-142.

Geertsen, K. S. K. N. R. &. S. P., 2020. APPLYING XBEACH ON 7,300 KM COAST: COASTAL CLIFF RETREAT DURING A STORM.. Coastal Engineering Proceedings, (36v), pp. 6-6..

Hallin, C. o.a., 2021. A comparative study of the effects of the 1872 storm and coastal flood risk management in Denmark, Germany, and Sweden. Water 13, 12, p. 1697.

Hanson, H. & Larson, M., 2008. Implications of extreme waves and water levels in the southern Baltic Sea. Journal of Hydraulic Research, 46(S2), pp. 292-302.

Hashemi, M., Neill, S. & Davies, A., 2015. A coupled tide-wave model for the NW European shelf seas.. Geophysical and Astrophysical Fluid Dynamics, 109(3), pp. 234-243.

Hersbach, H. o.a., 2020. The ERA5 global reanalysis.. Quarterly Journal of the Royal Meteorological Society, 146(730), pp. 1999-2049.

Hofstede, J. & Hamann, M., 2022. The 1872 catastrophic storm surge at the Baltic Sea coast of Schleswig-Holstein; lessons learned?. Die Küste, 10, p. 1.092101.

Hünicke, B. o.a., 2015. Chapter 9: Sea Level and Wind Waves, Secon Assessment of Climate Change for the Baltic Sea Basin. i: u.o.:the BACC II Author team.

Jensen, J. & Müller-Navarra, S. H., 2008. Storm Surges on the German Coast. Die Küste, 74 ICCE, pp. 92-124.

Malmberg-Persson, K., Nyberg, J., Ising, J. & Rodhe, L., 2016. Skånes känsliga stränder – erosionsförhållanden och geologi för samhällsplanering, u.o.: SGU-report.

Pallares, E., Sánchez-Arcilla, A. & Espino, M., 2014. Wave energy balance in wave models (SWAN) for semi-enclosed domains-Application to the Catalan coast. Continental Shelf Research, 87, pp. 41-53.

Rosenhagen, G. & Bork, I., 2009. Rekonstruktion der Sturmflutwetterlage vom 13. November 1872. Die Küste, 75, pp. 51-70.

Rusu, L., Pilar, P. & Guedes Soares, C., 2008. Hindcast of the wave conditions along the west Iberian coast. Coastal Engineering, 55(11), pp. 906-919.

Sukchaiwan, E., 2023. Dune Erosion on the Falsterbo Peninsula, Delft: u.n.

Vousdouskas, M. I. F. V. M. I. F. Ó. A. L. P. &. P. A., 2012. Toward reliable storm-hazard forecasts: XBeach calibration and its potential application in an operational early-warning system.. Ocean Dynamics, 62, pp. 1001-1015..